

Neutral and Cationic Molybdenum Imido Alkylidene Cyclic Alkyl Amino Carbene (CAAC) Complexes for Olefin Metathesis

Koushani Kundu,^[a] Janis V. Musso,^[a] Mathis J. Benedikter,^[a] Wolfgang Frey,^[b] Katrin Gugeler,^[c] Johannes Kästner,^[c] and Michael R. Buchmeiser^{*[a, d]}

The first neutral and cationic Mo imido alkylidene cyclic alkyl amino carbene (CAAC) complexes of the general formulae $[\text{Mo}(\text{N}-\text{Ar})(\text{CHCMe}_2\text{Ph})(\text{X})_2(\text{CAAC})]$ and $[\text{Mo}(\text{N}-\text{Ar})(\text{CHCMe}_2\text{Ph})(\text{X})(\text{CAAC})][\text{B}(\text{Ar}^f)_4]$ ($\text{X}=\text{Br}, \text{Cl}, \text{OTf}, \text{OC}_6\text{F}_5$; $\text{CAAC} = 1-(2,6\text{-iPr}_2\text{-C}_6\text{H}_3)\text{-}3,3,5,5\text{-tetramethyltetrahydropyrrol-}2\text{-ylidene}$) have been synthesized from molybdenum imido bishalide alkylidene DME precursors. Different combinations of the imido and "X" ligands have been employed to understand synthetic peculiarities. Selected complexes have been characterized by single-crystal X-ray analysis. Due to the pronounced σ -donor/ π -acceptor characteristics of CAACs, the corresponding neutral and cationic molybdenum imido alkylidene CAAC complexes do not require the presence of stabilizing donor

ligands such as nitriles. Calculations on the PBE0-D3BJ/def2-TZVP level for PBE0-D3BJ/def2-SVP optimized geometries revealed partial charges at molybdenum similar to the corresponding molybdenum imido alkylidene *N*-heterocyclic carbene (NHC) complexes with a slightly higher polarization of the molybdenum alkylidene bond in the CAAC complexes. All cationic complexes have been tested in olefin metathesis reactions and showed improved activity compared to the analogous NHC complexes for hydrocarbon-based substrates, allowing for turnover numbers (TONs) up to 9500 even at room temperature. Some Mo imido alkylidene CAAC complexes are tolerant towards functional groups like thioethers and sulfonamides.

Introduction

Pioneered by the groups of Schrock et al.^[1] and Grubbs et al.,^[2] a remarkable collection of metal catalysts for different types of olefin metathesis reactions has been created over the past few decades. Complementary, Basset et al.^[3] and Copéret et al.^[4] elucidated the role of the support and the specific advantages of surface organometallic chemistry with immobilized, well-defined organometallic catalysts. The chemistry of group 6 metal alkylidene NHC complexes was also researched by our

group.^[5] Many years of research on ligand design in organometallic catalysis have shown that fine-tuning the ligand systems enables for higher reactivity, minimal catalyst loading, and better selectivity.


Cyclic alkyl amino carbenes (CAACs) were first reported in 2005^[6] and are regarded as a favored group of ligands in transition metal catalysis. They have attracted substantial attention due to their electronic characteristics, which are distinctively different from those of conventional *N*-heterocyclic carbenes (NHCs). In particular the more pronounced σ -donor and π -acceptor capabilities compared to NHCs^[7] make them highly attractive as ligands in organometallic catalysis. Indeed, some transition metal CAAC complexes showed remarkable catalytic activity. For instance, Gao et al. were able to achieve Markovnikov hydrofunctionalization of terminal alkynes with a wide variety of substrates using Cu-CAAC catalysts.^[8] In 2021, Proetto et al. revealed that the anti-cancer activity of Au-CAAC complexes stems from the unique electronic properties and coordination environment offered by CAACs.^[9] In addition, Ru-based Grubbs-type catalysts bearing CAACs showed high productivity in olefin metathesis reactions.^[2a,10] In view of that, we were interested in investigating synthetic strategies to gain access to Mo-based CAAC complexes and in exploring their structural characteristics and use in olefin metathesis. In this work we present a series of neutral and cationic molybdenum imido alkylidene CAAC complexes of the general formulae $[\text{Mo}(\text{N}-\text{Ar})\text{X}_2(\text{CHCMe}_2\text{Ph})(\text{CAAC})]$ and $[\text{Mo}(\text{N}-\text{Ar})\text{X}(\text{CHCMe}_2\text{Ph})(\text{CAAC})][\text{B}(\text{Ar}^f)_4]$, respectively, based on different imido and anionic "X" ligands along with selected single crystal X-ray structures. Finally, their use in olefin homometathesis


[a] K. Kundu, Dr. J. V. Musso, Dr. M. J. Benedikter, Prof. Dr. M. R. Buchmeiser
Institute of Polymer Chemistry
University of Stuttgart
Pfaffenwaldring 55, 70569 Stuttgart (Germany)
E-mail: michael.buchmeiser@ipoc.uni-stuttgart.de

[b] Dr. W. Frey
Institute of Organic Chemistry
University of Stuttgart
Pfaffenwaldring 55, 70569 Stuttgart (Germany)

[c] K. Gugeler, Prof. Dr. J. Kästner
Institute of Theoretical Chemistry
University of Stuttgart
Pfaffenwaldring 55, 70569 Stuttgart (Germany)

[d] Prof. Dr. M. R. Buchmeiser
German Institutes of Textile and Fiber Research (DITF)
Körschtalstr. 26, 73770 Denkendorf (Germany)

 Supporting information for this article is available on the WWW under <https://doi.org/10.1002/chem.202301818>

 © 2023 The Authors. Chemistry - A European Journal published by Wiley-VCH GmbH. This is an open access article under the terms of the Creative Commons Attribution License, which permits use, distribution and reproduction in any medium, provided the original work is properly cited.

(HM) and ring-closing olefin metathesis (RCM) reactions with various substrates is reported.

Results and Discussion

Synthesis of neutral Mo CAAC complexes

The bistriflate route^[11] has been widely acknowledged in previous decades as a means of gaining access to a large library of neutral Mo imido alkylidene complexes.^[5cd] Although this route allows for introducing a variety of alkoxide and NHC ligands, it has significant drawbacks, such as the difficulty of the corresponding Mo-bistriflate complexes to bind strongly basic carbene ligands like CAACs. Indeed, CAACs with low TEPs tend to irreversibly deprotonate the alkylidene moiety resulting in the formation of metal alkylidynes. Therefore, the synthesis of Mo imido alkylidene CAAC complexes from the corresponding Mo-bistriflate complexes turned out to be difficult. Thus, the attempt to coordinate 1-(2,6-*i*Pr₂-C₆H₃)-3,3,5,5-tetramethyltetrahydropyrrol-2-ylidene (CAAC) with a TEP of 2046 cm⁻¹^[12] directly to [Mo(N-2,6-*i*Pr₂-C₆H₃)(OTf)₂(CHCMe₂Ph)DME] (**Mo1**, Scheme 1) resulted only in low conversion (~10%); longer reaction times resulted in the full decomposition of the complex. We therefore focused on molybdenum imido alkylidene bromide and chloride complexes as appropriate substitutes. Our group already reported on neutral and cationic tungsten bromo alkylidene NHC complexes that exhibit promising olefin metathesis activity.^[13] The corresponding cationic molybdenum imido alkylidene NHC complexes, however, showed poor stability and were only isolable in the presence of a coordinating solvent like acetonitrile.^[14]

We were therefore interested in the question whether CAACs can stabilize the cationic halide complexes to make them isolable in crystalline form in order to gain more insight about the structural characteristics of this new group of

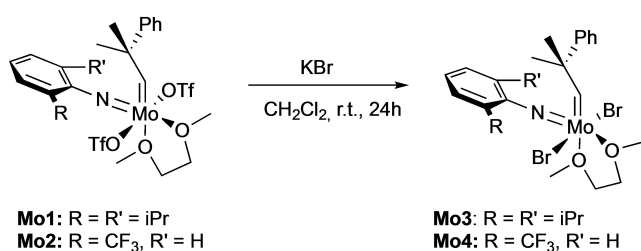
complexes. Following the reported procedure,^[14] the corresponding dibromo progenitors were easily accessible by treating the corresponding bistriflate imido alkylidene precursors with excess KBr (Scheme 1). The molybdenum imido dichloro alkylidene complex [Mo(N-2-*t*Bu-C₆H₄)Cl₂(CHCMe₂Ph)DME] (**Mo6**) was synthesized by reacting an ethereal HCl solution with the bispyrrolide complex [Mo(N-2-*t*Bu-C₆H₄)(pyr)₂(CHCMe₂Ph)] (**Mo5**).^[15] The dibromo complex [Mo(N-2-CF₃-C₆H₄)Cl₂(CHCMe₂Ph)DME] (**Mo4**) is literature known,^[14] whereas to the best of our knowledge [Mo(N-2,6-*i*Pr₂-C₆H₃)Cl₂(CHCMe₂Ph)DME] (**Mo3**) and **Mo6** have not yet been reported.

Addition of a solution of free CAAC in benzene to the corresponding molybdenum imido alkylidene dihalide precursors proceeded smoothly and CAAC replaced DME to produce the first neutral molybdenum imido alkylidene CAAC complexes **Mo7–Mo9** (Scheme 2).

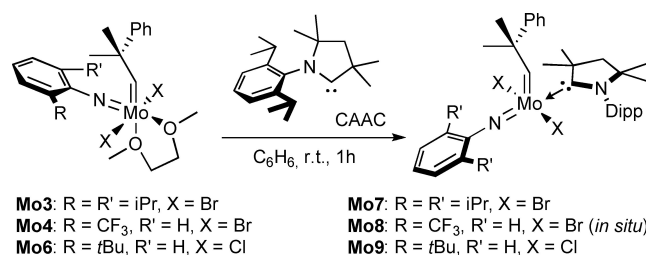
Crystalline samples of both [Mo(N-2,6-*i*Pr₂-C₆H₃)Br₂(CHCMe₂Ph)(CAAC)] (**Mo7**) and [Mo(N-2-*t*Bu-C₆H₄)Cl₂(CHCMe₂Ph)(CAAC)] (**Mo9**), suitable for single-crystal X-ray analysis, were obtained (Figure 2, Figure 3). However, **Mo8**'s poor solubility in common solvents prevented its isolation in crystalline form; therefore, it was used as obtained for further reaction.

Synthesis of cationic Mo CAAC complexes

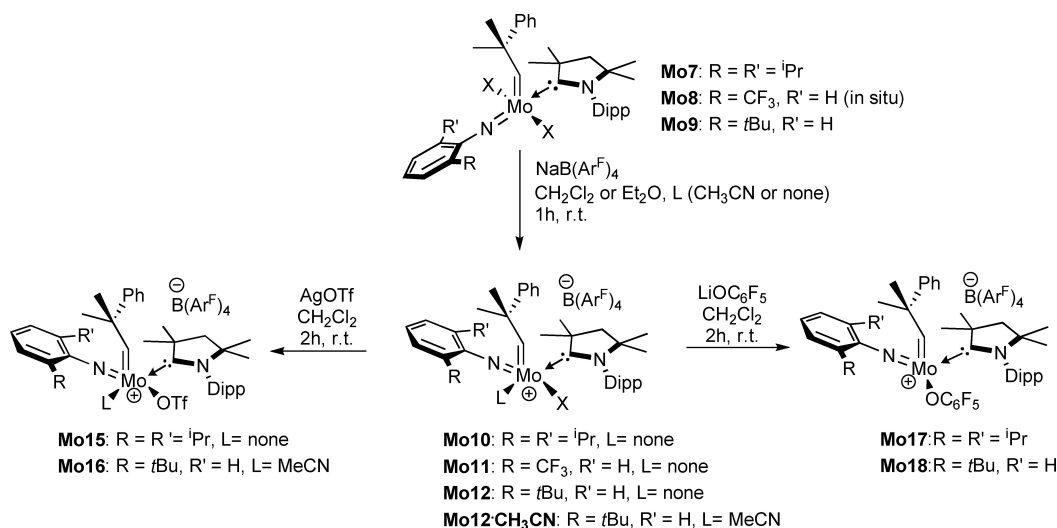
The synthesis of the corresponding cationic complexes was carried out by replacing one halide in complexes **Mo7–Mo9** by a bulky and weakly coordinating anion, i.e. tetrakis(3,5-(CF₃)₂-C₆H₃)borate (= B(Ar^F)₄, Scheme 3). Complexes **Mo10–Mo12** were obtained in isolated yields of 75%, 72% and 87%, respectively. As outlined above, so far one single cationic molybdenum imido alkylidene monohalide NHC complex, [Mo(N-2-CF₃-C₆H₄)Br(CHCMe₂Ph)(6-Mes)(MeCN)₂][B(Ar^F)₄] (**Mo14**)^[14] has been reported (Figure 1), which was indeed only isolable with two molecules of acetonitrile coordinated to the metal. Moreover, it decomposed in solution. Even though cationic molybdenum imido alkylidene monohalide CAAC complexes were isolable without any coordinating solvent, still, a few drops of acetonitrile were added to a solution of [Mo(N-2-*t*Bu-C₆H₄)Cl(CHCMe₂Ph)(CAAC)][B(Ar^F)₄] (**Mo12**) in CH₂Cl₂ to see if there was any room for the coordination of acetonitrile.



Scheme 1. Synthesis of the molybdenum dibromo precursors **Mo3–Mo4** and the molybdenum dichloro-precursor **Mo6**.



Scheme 2. Synthesis of neutral molybdenum CAAC complexes **Mo7–Mo9** from the bishalide precursors **Mo3–Mo4** and **Mo6**.



Scheme 3. Synthesis of cationic molybdenum imido alkylidene CAAC complexes and subsequent salt metathesis.

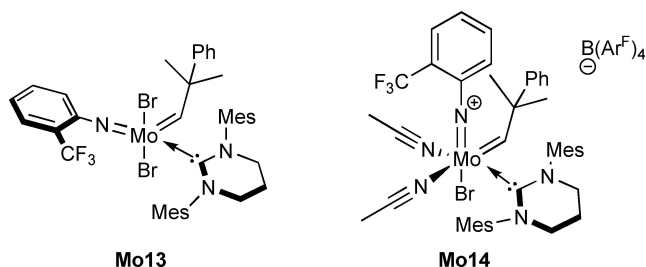


Figure 1. Neutral and cationic molybdenum bromo alkylidene NHC complexes **Mo13** and **Mo14**.^[14]

An observable color change from bright yellow to pale orange was noticed. The resulting [Mo(N-2-^tBu-C₆H₄)Cl-(CHCMe₂Ph)(CAAC)(CH₃CN)][(B(Ar^F)₄)⁺] (**Mo12CH₃CN**) was easily crystallizable for single-crystal X-ray analysis (Figure 6). Our research has previously found that Mo or W complexes with stronger electron-withdrawing ligands, such as alkoxides or triflates, display higher olefin metathesis productivities.^[5b,13, 16] Since we could not coordinate the CAAC directly to the bistriflate precursor [Mo(N-2-CF₃-C₆H₄)(OTf)₂(CHCMe₂Ph)DME] (**Mo2**), salt metathesis of the corresponding halide complex was considered a suitable alternative pathway. And indeed, [Mo(N-2,6-ⁱPr₂-C₆H₃)(OTf)(CHCMe₂Ph)(CAAC)][(B(Ar^F)₄)⁺] (**Mo15**) and [Mo(N-2-^tBu-C₆H₄)(OTf)(CHCMe₂Ph)(CAAC)(CH₃CN)][(B(Ar^F)₄)⁺] (**Mo16**) were obtained by treating [Mo(N-2,6-ⁱPr₂-C₆H₃)Br-(CHCMe₂Ph)(CAAC)][(B(Ar^F)₄)⁺] (**Mo10**) and **Mo12CH₃CN** with AgOTf. Similarly, salt metathesis with LiOC₆F₅ resulted in the formation of [Mo(N-2,6-ⁱPr₂-C₆H₃)(CHCMe₂Ph)(OC₆F₅)(CAAC)][(B(Ar^F)₄)⁺] (**Mo17**) and [Mo(N-2-^tBu-C₆H₄)(CHCMe₂Ph)(OC₆F₅)(CAAC)][(B(Ar^F)₄)⁺] (**Mo18**), respectively. For steric reasons, the acetonitrile does not remain coordinated to the metal center in **Mo18**. Also, no reaction was observed between **Mo10** and bulky lithium 2,6-diphenylphenoxide. Possibly, the higher steric bulk of the CAAC does not provide enough space for the bulky 2,6-diphenylphenoxide to replace the bromide.

Single-crystal X-ray crystallography

To confirm the structures and gain more insight into the structural peculiarities of the new CAAC complexes, representative complexes were subjected to single crystal X-ray analysis. For all measurements, thermal ellipsoids were set to a 50% probability level.

Mo7 (Figure 2) crystallizes in the triclinic space group $P\bar{1}$ with $a = 1187.51(7)$ pm, $b = 1285.49(8)$ pm, $c = 1413.08(8)$ pm, $\alpha = 69.275(2)^\circ$, $\beta = 87.256(3)^\circ$, $\gamma = 80.988(3)^\circ$, $Z = 2$. Molybdenum adopts a slightly distorted square-pyramidal (SP) geometry ($\tau_5^{[17]} = 0.13$) with the alkylidene ligand in the apex. **Mo9** (Figure 3) also crystallizes in the triclinic space group $P\bar{1}$ with $a = 1152.50(10)$ pm, $b = 1341.52(13)$ pm, $c = 1360.19(12)$ pm, $\alpha =$

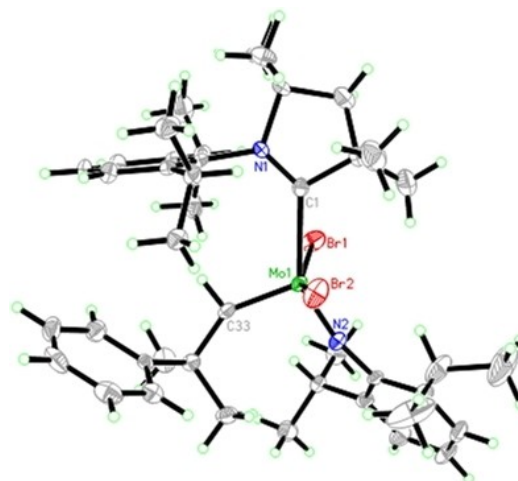


Figure 2. Single-crystal X-ray structure of **Mo7**. Relevant bond lengths [pm] and angles [°]: Mo(1)–N(2) 174.2(2), Mo(1)–C(33) 185.9(3), Mo(1)–C(1) 231.9(3), Mo(1)–Br(2) 254.30(3), Mo(1)–Br(1) 254.77(3); N(2)–Mo(1)–C(33) 102.46(10), N(2)–Mo(1)–C(1) 146.06(9), C(33)–Mo(1)–C(1) 111.29(10), N(2)–Mo(1)–Br(2) 96.41(6), C(33)–Mo(1)–Br(2) 96.60(7), C(1)–Mo(1)–Br(2) 83.60(6), N(2)–Mo(1)–Br(1) 91.39(6), C(33)–Mo(1)–Br(1) 106.04(7), C(1)–Mo(1)–Br(1) 76.19(6), Br(2)–Mo(1)–Br(1) 153.853(15).

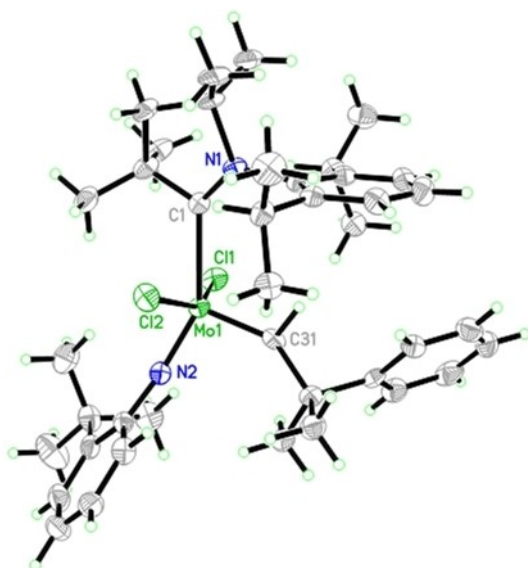


Figure 3. Single-crystal X-ray structure of **Mo9**. Relevant bond lengths [pm] and angles [°]: Mo(1)–N(2) 174.7(3), Mo(1)–C(31) 185.2(4), Mo(1)–C(1) 235.5(4), Mo(1)–Cl(1) 237.63(10), Mo(1)–Cl(2) 240.93(10); N(2)–Mo(1)–C(31) 99.17(17), N(2)–Mo(1)–C(1) 149.79(15), C(31)–Mo(1)–C(1) 109.51(16), N(2)–Mo(1)–Cl(1) 99.62(10), C(31)–Mo(1)–Cl(1) 100.54(11), C(1)–Mo(1)–Cl(1) = 84.61(9), N(2)–Mo(1)–Cl(2) 88.71(10), C(31)–Mo(1)–Cl(2) 104.62(11), C(1)–Mo(1)–Cl(2) 75.31(9), Cl(1)–Mo(1)–Cl(2) 151.86(4).

63.661(5)°, β = 87.415(5)°, γ = 85.573(4)°, Z = 2. The metal adopts an almost ideal SP geometry (τ_5 = 0.03). The metal-carbene bonds for **Mo7** and **Mo9** (231.9 pm and 235.4 pm, respectively) are noticeably longer than in previously reported neutral Mo-NHC complexes (219–224 pm).^[5c] However, they are in the same range as in **Mo13** (234.8 pm),^[14] which makes us consider this longer Mo–C(carbene) bond a structural characteristic of dihalide Mo imido alkylidene complexes. Even though **Mo13** adapts a geometry in between SP and trigonal bipyramidal (TBP), **Mo7** and **Mo9** are almost perfectly SP due to the smaller N–C_{NHC}–C bond angle in the CAAC compared to the N–C_{NHC}–N bond angle in a 6-membered cyclic NHC. All tetra-coordinated cationic complexes adopt a distorted tetrahedral geometry, whereas the cationic complexes with coordinated solvent molecules acquire a geometry between SP and TBP.

Mo10 (Figure 4) crystallizes in monoclinic space group $P2_1/c$ with a = 1831.26(9) pm, b = 2042.81(8) pm, c = 2281.92(10) pm, α = γ = 90°, β = 100.921(2)°, Z = 4, with distorted tetrahedral geometry (τ_4 = 0.82). **Mo11** (Figure 5) crystallizes in monoclinic space group $P2_1/c$ with a = 2124.13(16) pm, b = 2102.66(17) pm, c = 1925.13(16) pm, α = γ = 90°, β = 97.731(5)°, Z = 4 with a disordered Br moiety attached to Mo on alternative positions with a distribution of 2:1 (Supporting Information, Figure S37). It acquires tetrahedral geometry with τ_4 = 0.811. Pentacoordinated **Mo12**·CH₃CN (Figure 6) crystallizes in the monoclinic space group $P2_1/c$ with a = 1394.89(6) pm, b = 2745.83(12) pm, c = 1914.36(9) pm, α = γ = 90°, β = 95.726(2)°, Z = 4. The metal adopts a geometry in between SP and TBP (τ_4 = 0.45).

Mo15 (Figure 7) adopts tetrahedral geometry with τ_4 = 0.79 and crystallizes in the triclinic space group $P\bar{1}$ with a = 1185.38(6) pm, b = 1641.02(7) pm, c = 2102.95(8) pm, α =

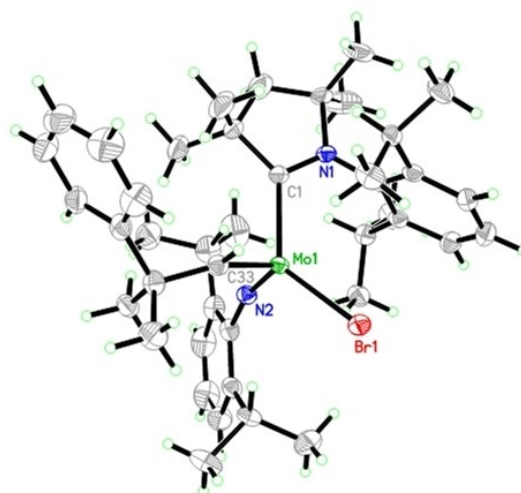


Figure 4. Single-crystal X-ray structure of **Mo10**. Relevant bond lengths [pm] and angles [°]: Mo(1)–N(2) 172.6(2), Mo(1)–C(33) 187.5(3), Mo(1)–C(1) 220.1(3), Mo(1)–Br(1) 246.05(4); N(2)–Mo(1)–C(33) 101.77(12), N(2)–Mo(1)–C(1) 101.75(11), C(33)–Mo(1)–C(1) 99.51(12), N(2)–Mo(1)–Br(1) 114.00(8), C(33)–Mo(1)–Br(1) 106.54(9), C(1)–Mo(1)–Br(1) 129.34(8). Anion omitted for clarity.

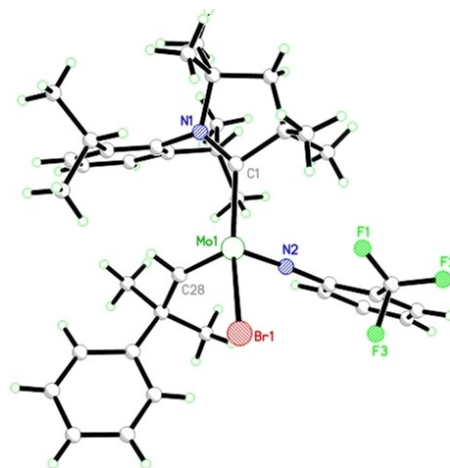


Figure 5. Single-crystal X-ray structure of **Mo11**. Relevant bond lengths [pm] and angles [°]: Mo(1)–N(2) 171.2(7), Mo(1)–C(28) 187.8(11), Mo(1)–C(1) 223.1(10), Mo(1)–Br(1 A) 251.3(2), Mo(1)–Br(1) 258.80(17); N(2)–Mo(1)–C(28) 103.0(4), N(2)–Mo(1)–C(1) 98.4(4), C(28)–Mo(1)–C(1) 106.1(4), N(2)–Mo(1)–Br(1 A) 147.4(3), C(28)–Mo(1)–Br(1 A) 109.4(3), C(1)–Mo(1)–Br(1 A) 75.9(2), N(2)–Mo(1)–Br(1) 91.3(3), C(28)–Mo(1)–Br(1) 94.1(3), C(1)–Mo(1)–Br(1) 154.8(2). Anions omitted for clarity.

101.348(2)°, β = 100.455(2)°, γ = 91.479(2)°, Z = 2. **Mo16** (Figure 8) crystallizes in the monoclinic space group $P2_1/c$ with a = 2187.83(11) pm, b = 1879.44(11) pm, c = 2000.02(10) pm, α = γ = 90°, β = 109.576(3)°, Z = 4. The metal shows a geometry in between SP and TBP with τ_4 = 0.5. The Mo–O(triflate) bond in **Mo16** is much longer (214.5 pm) compared to the one in **Mo15** (204.19 pm).

A similar difference was also observed between the tetra- and pentacoordinated cationic Mo triflate NHC complexes [Mo(N-2,6-Cl₂-C₆H₃)(CHCMe₃)(IMes)(OTf)][B(Ar^F)₄] and [Mo(N-2,6-F₂-C₆H₃)(CHCMe₂Ph)(IMes)(OTf)(CH₃CN)][B(Ar^F)₄]^[18] with bond

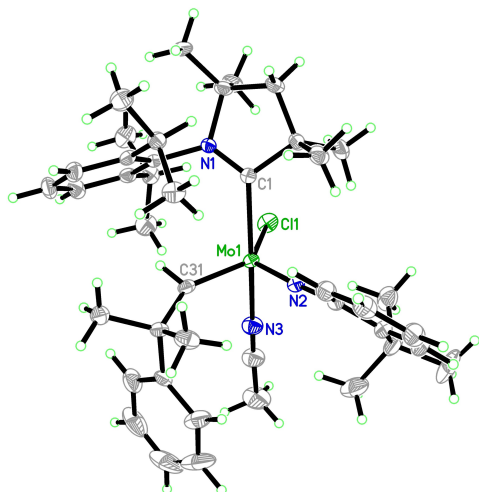


Figure 6. Single-crystal X-ray structure of **Mo12CH₃CN**. Relevant bond lengths [pm] and angles [°]: Mo(1)–N(2) 172.32(19), Mo(1)–C(31) 189.4(2), Mo(1)–N(3) 218.0(2), Mo(1)–C(1) 222.9(2), Mo(1)–Cl(1) 240.87(6); N(2)–Mo(1)–C(31) 102.23(9), N(2)–Mo(1)–N(3) 96.84(9), C(31)–Mo(1)–N(3) 86.81(9), N(2)–Mo(1)–C(1) 102.05(8), C(31)–Mo(1)–C(1) 103.76(8), N(3)–Mo(1)–C(1) 155.70(8), N(2)–Mo(1)–Cl(1) 128.21(7), C(31)–Mo(1)–Cl(1) 128.54(7), N(3)–Mo(1)–Cl(1) 78.62(6), C(1)–Mo(1)–Cl(1) 77.71(5). Anion omitted for clarity.

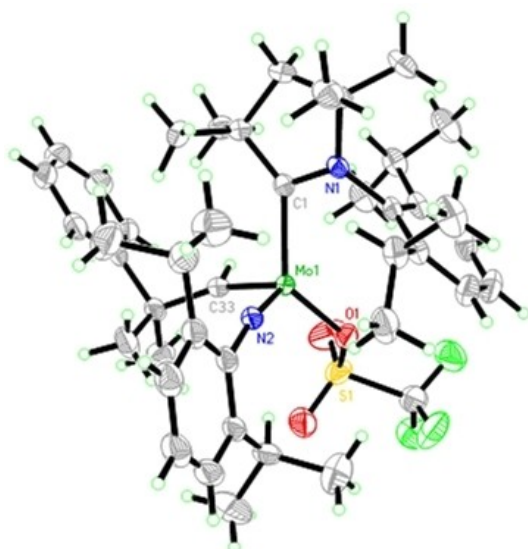


Figure 7. Single-crystal X-ray structure of **Mo15**. Relevant bond lengths [pm] and angles [°]: Mo(1)–N(2) 171.2(2), Mo(1)–C(33) 186.7(2), Mo(1)–O(1) 204.19(17), Mo(1)–C(1) 218.5(2); N(2)–Mo(1)–C(33) 100.42(10), N(2)–Mo(1)–O(1) 116.53(9), C(33)–Mo(1)–O(1) 101.85(9), N(2)–Mo(1)–C(1) 100.41(9), C(33)–Mo(1)–C(1) 99.91(9) O(1)–Mo(1)–C(1) 132.21(8). Anion omitted for clarity.

lengths of 217.9 pm and 208.9 pm, respectively. The Mo–O (triflate) bond length, however, is shorter in the penta-coordinated complex than it is in the tetra-coordinated one, reversing the pattern seen in CAAC complexes. Notably, the tetra-coordinated cationic molybdenum center in [Mo(N-2,6-Cl₂-C₆H₃)(CHCMe₃)(IMes)(OTf)][B(Ar^F)₄]^[18] shows η²-binding of the triflate ligand in the absence of an additional coordinating solvent. However, no such coordination was observed in the analogous CAAC complexes, irrespective of the absence of

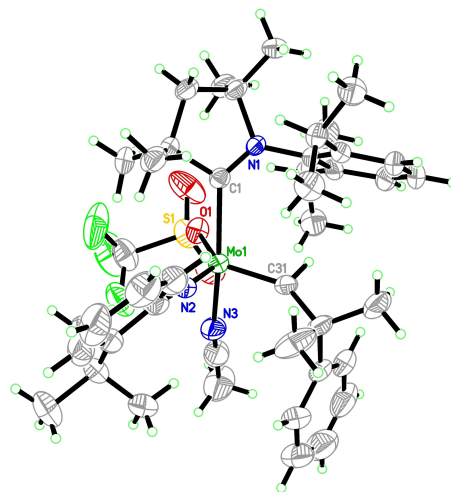


Figure 8. Single-crystal X-ray structure of **Mo16**. Relevant bond lengths [pm] and angles [°]: Mo(1)–N(2) 171.8(3), Mo(1)–C(31) 186.5(4), Mo(1)–O(1) 214.5(3), Mo(1)–N(3) 217.6(4), Mo(1)–C(1) 222.7(4); N(2)–Mo(1)–C(31) 99.94(18), N(2)–Mo(1)–O(1) 135.19(14), C(31)–Mo(1)–O(1) 124.40(15), N(2)–Mo(1)–N(3) 99.87(16), C(31)–Mo(1)–N(3) 87.71(16), O(1)–Mo(1)–N(3) 77.83(13), N(2)–Mo(1)–C(1) 101.16(14), C(3)–Mo(1)–C(1) 103.43(15), O(1)–Mo(1)–C(1) 76.52(12), N(3)–Mo(1)–C(1) 154.02(15). Anion omitted for clarity.

coordinated acetonitrile. Clearly, the CAAC has a stronger stabilizing effect, which eliminates the need for a second interaction with the triflate ligand.

Mo18 (Figure 9) crystallizes in the triclinic space group $P\bar{1}$ with $a = 1300.81(13)$ pm, $b = 1573.91(16)$ pm, $c = 1929.3(2)$ pm, $\alpha = 91.483(5)^\circ$, $\beta = 105.370(5)^\circ$, $\gamma = 90.383(4)^\circ$, $Z = 2$. The metal adopts a tetrahedral geometry ($\tau_4 = 0.83$). Despite the higher theoretical σ -donor and π -accepting ability of the CAAC ligand, no major structural differences were observed in the molybdenum carbene bond lengths of Mo–NHC and Mo–CAAC complexes.

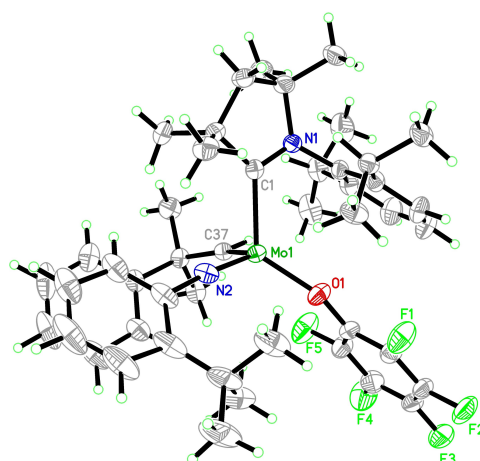


Figure 9. Single-crystal X-ray structure of **Mo18**. Relevant bond lengths [pm] and angles [°]: Mo(1)–N(2) 171.19(17), Mo(1)–C(37) 187.38(18), Mo(1)–O(1) 192.21(14), Mo(1)–C(1) 215.99(19); N(2)–Mo(1)–C(37) 102.21(8), N(2)–Mo(1)–O(1) 117.84(8), C(37)–Mo(1)–O(1) 113.11(7), N(2)–Mo(1)–C(1) 103.06(8), C(37)–Mo(1)–C(1) 91.53(7), O(1)–Mo(1)–C(1) 124.24(7). Anion omitted for clarity.

Calculations

For a more detailed inspection of the charge distribution of a cationic Mo-CAAC (**Mo-16**) and Mo-NHC (**Mo-19**,^[5e] Figure 10) complex the atomic charges were calculated for both complexes.

Calculations were performed at the PBE0-D3BJ/def2-TZVP level for PBE0-D3BJ/def2-SVP optimized geometries with the charge model 5 (CM5) analogously to previous calculations for cationic molybdenum imido alkylidene NHC complexes.^[5b,h] It is important to mention that these calculated charges are not physical observables and should not be overinterpreted as approximations for oxidation states. Indeed, different charge

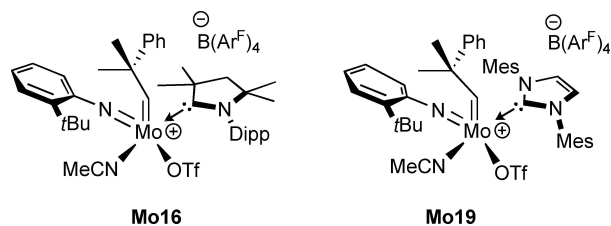


Figure 10. Structurally related molybdenum imido alkylidene CAAC and NHC complexes **Mo16** and **Mo19**.^[5e]

	Mo-16	Mo-19
Mo	1.335	1.330
Mo=C _{HR}	-0.258	-0.252
Mo=C _{HR}	0.096	0.105
polarization Mo=C _{HR}	1.593	1.582
alkylidene	-0.033	-0.034
CAAC/NHC	0.393	0.445
Imido	-0.341	-0.363
Triflate	-0.464	-0.495
MeCN	0.111	0.116

models lead to slightly different numbers; however, the same conclusions can be drawn (Supporting Information). Calculations revealed that the partial charge at the metal center is comparable for both complexes (1.335 e for **Mo-16** vs. 1.330 e for **Mo-19**, Table 1).

With the charge of the carbon of the alkylidene ligand also being similar for both complexes (-0.252 e vs. -0.258 e), the polarization of the Mo=C bond is only slightly higher for **Mo-16** than in **Mo-19** (1.593 e vs. 1.582 e). These polarizations and partial charges are comparable to those of the Mo-complexes reported earlier.^[5h] The partial charge of the alkylidene fragment is the same for both complexes. The CAAC ligand and the NHC ligand both have a positive partial charge, which indicates an electron donation and therefore stabilization of the metal center. However, the partial charge of the NHC ligand (0.445 e) in **Mo-19** is significantly higher than of the CAAC ligand (0.393 e) in **Mo-16**. The negative partial charges of the imido ligand and triflate ligand being slightly higher in **Mo-19** (-0.363 e and -0.495 e vs. -0.341 e and -0.464 e) indicates a more pronounced electron donation from the NHC ligand in **Mo-19** compared to the CAAC ligand in **Mo-16**. The partial charge of the acetonitrile ligand is comparable for both complexes.

Reactivity in olefin metathesis

The novel CAAC complexes were benchmarked in a series of ring-closing olefin metathesis (RCM) and homometathesis (HM) reactions (Table 2). For the HM of 1-octene, catalysts **Mo10–Mo12** and **Mo15–Mo18** showed good to high productivity, resulting in turnover numbers (TONs) of up to 2480, which translates into 95% yield. Similar was observed in the RCM of 1,7-octadiene, high productivity was observed, the only exception being **Mo12** and **Mo12/MeCN**. Since **Mo15** and **Mo17** showed practically full conversion for both substrates, they were further tested with a lower catalyst loading of 0.01 mol%. Both complexes were highly active and allowed for high yields (>90%) translating into TONs up to 9500. Clearly, these CAAC

Substrate	Mo10	Mo11	Mo12	Mo12/CH ₃ CN	Mo15	Mo16	Mo17	Mo18
Ring closing metathesis (RCM)								
1,7-Octadiene	2500	1330	450	430	2500	2350	2460	1900
Diallyl sulfide	0	0	0	0	120	130	450	520
N,N-Diallyl-4-methyl-benzenesulfonamide	190	100	70	50	200	225	330	380
Homometathesis (HM)								
1-Octene	2200 (95)	1310 (79)	1930 (78)	1850 (78)	2480 (85)	2400 (79)	2420 (94)	2420 (79)
Allylbenzene	260 (99)	330 (80)	190 (91)	190 (91)	385 (79)	1370 (90)	0	510 (96)
Allyltrimethylsilane	160	1550	400	300	790	300	200	140

[a] Reaction conditions: Catalyst: substrate = 1:2500, Solvent: 1,2-dichloroethane, 4 h, room temperature, open vial. Internal standard: *n*-dodecane. Conversion determined by GC. Numbers in the parenthesis: % *E*-isomer. [b] Catalyst: substrate = 1:10000.

complexes outperform the structurally related molybdenum imido alkylidene NHC catalysts in terms of productivity with hydrocarbon-based olefins.^[13]

Next, functional group tolerance was tested using the structurally related molybdenum imido alkylidene CAAC and NHC complexes **Mo19** and **Mo16**. In contrast to **Mo19**, which was inactive in the RCM of diallyl sulfide and displayed a TON of 1100 in the HM of 1-octene,^[13] **Mo16** showed still some activity for diallyl sulfide (TON = 130) and almost full conversion for 1-octene (TON = 2400). Generally, complexes bearing electron-withdrawing pentafluorophenoxide ligands were most tolerant towards functional groups while halide complexes showed very low reactivity. The only exception was allyltrimethylsilane for which **Mo11** showed rather high activity with 60% conversion. Notably, unlike the NHC complexes,^[18] the CAAC complexes reported here were not active in olefin metathesis reactions of substrates containing protic functional groups such as alcohols or secondary amines.

Conclusions

Molybdenum imido alkylidene CAAC complexes add to the armory of metal alkylidene carbene complexes, the majority of which are built on NHCs. Alongside, we also explored robust molybdenum imido bishalide alkylidene precursors as alternatives to the standard bistriflate precursors. The absence of any secondary metal-triflate interaction (η^2 -binding) in the triflate complexes as well as the absence of coordinating solvents in the cationic halide complexes both suggest that CAACs can stabilize the corresponding complexes even more efficiently than NHCs. The novel molybdenum imido alkylidene CAAC complexes outperform the corresponding NHC complexes both in the HM and RCM of hydrocarbon-based olefins. In analogy to molybdenum imido alkylidene NHC complexes, increased functional group tolerance might be realized by introducing an electron-deficient imido group, yet this remains a challenging task.

Experimental Section

General: Unless stated otherwise, all reactions were performed under N₂ atmosphere either with standard Schlenk techniques or in a glovebox (LabMaster 130, MBraun, Garching, Germany). Glassware was stored at 120 °C overnight and cooled in an evacuated antechamber. CH₂Cl₂, diethyl ether, toluene, pentane, and tetrahydrofuran (THF) were dried by a solvent purification system (SPS, MBraun). Anhydrous benzene was purchased from Merck (Darmstadt, Germany) and stored over 4 Å molecular sieves. 1,2-Dimethoxyethane (DME) and 1,2-dichloroethane were distilled from CaH₂ prior to use and stored over 4 Å Linde type molecular sieves inside the glovebox. All substrates used for catalysis testing were passed through aluminum oxide and stored over 4 Å Linde-type molecular sieves prior to use. Starting materials and reagents were purchased from Merck (Darmstadt, Germany), Alfa Aesar (Karlsruhe, Germany), or ABCR (Karlsruhe, Germany) and were used as received unless stated otherwise. ¹H NMR and ¹⁹F NMR measurements were carried out on a Bruker Avance III 400 at 400 MHz and 376 MHz, respectively. ¹³C NMR spectra were recorded at the Institute of

Organic Chemistry, University of Stuttgart on a Bruker Avance III HD at 176 MHz using broadband decoupling. Chemical shifts are reported in ppm relative to the solvent signal. Data are reported as follows: chemical shift, multiplicity (s = singlet, d = doublet, t = triplet, q = quartet, quint = quintet, sept = septet, br = broad, m = multiplet), coupling constants (Hz) and integral. Single-crystal X-ray analysis was performed on a Bruker Kappa APEXII Duo diffractometer with Mo K α irradiation at the Institute of Organic Chemistry, University of Stuttgart, Germany. **Mo1**,^[11] **Mo2**,^[11] **Mo4**,^[14] **Mo5**,^[16] were synthesized according to literature procedures. **CAAC**^[19] was synthesized using a slightly modified literature procedure, contained one equivalent of HMDS, and was used as obtained.

Deposition Numbers 2261878 (**Mo7**), 2261879 (**Mo9**), 2261880 (**Mo10**), 2261881 (**Mo11**), 2261882 (**Mo12**CH₃CN), 2261883 (**Mo15**), 2261884 (**Mo16**), 2261885 (**Mo18**) contain the supplementary crystallographic data for this paper. These data are provided free of charge by the joint Cambridge Crystallographic Data Centre and Fachinformationszentrum Karlsruhe Access Structures service.

[Mo(N-2,6-*i*Pr₂-C₆H₃)(CHCMe₂Ph)Br₂DME] (Mo3): A solution of [Mo(N-2,6-*i*Pr₂-C₆H₃)(CHCMe₂Ph)(OTf)₂DME] (**Mo1**) (400 mg, 0.5 mmol, 1 equiv.) in CH₂Cl₂ was added to solid KBr (360 mg, 3.03 mmol, 6 equiv.). The suspension was stirred for 24 h at ambient temperature. The yellow suspension was filtered and the filtrate was dried *in vacuo*. The dark yellow foam was taken up in diethyl ether, filtered, concentrated and stored at -37 °C overnight to get shiny yellow crystals. Yield: 270 mg (82%). ¹H NMR (CDCl₃): δ 13.20 (s, 1H), 7.41 (d, 2H), 7.30 (t, J = 8, 2H), 7.22-7.15 (m, 2H), 7.10 (m, 2H), 4.40 (sept, J = 8, 2H), 4.02 (s, 4H), 3.72 (s, 6H), 1.60 (s, 6H), 1.20 (d, J = 4, 12H). ¹³C NMR (CDCl₃): δ 315.5, 151.9, 150.1, 149.8, 128.5, 128.3, 126.0, 123.9, 71.5, 65.8, 62.5, 57.3, 29.1, 28.1, 24.7, 15.3. Elemental Analysis Calculated for C₂₆H₃₃Br₂MoNO₂: C, 47.80; H, 6.02; N, 2.14; Found: C, 48.01; H, 6.02; N, 2.15.

[Mo(N-2-*t*BuC₆H₄)(CHCMe₂Ph)Cl₂DME] (Mo6): A cold (-35 °C) solution of HCl (2 M in diethyl ether, 3.33 mL, 6.66 mmol, 2 equiv.) was added to a cold (-35 °C) suspension of [Mo(N-2-*t*BuC₆H₄)(CHCMe₂Ph)(pyr)₂] (**Mo5**, 1.69 g, 3.33 mmol, 1 equiv.) in a mixture of DME (2 mL) and diethyl ether (40 mL). The reaction mixture was stirred at room temperature for 20 min during which time it turned into an orange suspension. The suspension was filtered and the solid was washed with cold diethyl ether (10 mL) to yield the product as a yellow solid. Another batch of product crystallized after concentrating the filtrate to ca. 6 mL and storing it at -35 °C overnight. Combined yield: 1.62 g (91%). ¹H NMR (C₆D₆): δ 13.13 (s, 1H), 8.82 (d, J = 6.6, 1H), 7.61 (d, J = 7.2, 2H), 7.26 (s, 2H), 7.12 (d, J = 8.0, 1H), 7.05 (t, J = 7.4, 1H), 6.94 (t, J = 7.6, 1H), 6.85 (t, J = 7.6, 1H), 3.16 (s, 10H), 1.81 (s, 6H), 1.70 (s, 9H); ¹³C NMR (C₆D₆): δ 307.6, 154.6, 151.5, 144.9, 131.6, 128.4, 128.4, 126.6, 126.1, 126.0, 125.7, 71.0, 61.3, 57.1, 35.7, 30.3, 29.8. Elemental Analysis (%) Calcd. for C₂₄H₃₅Cl₂MoNO₂: C 53.74, H 6.58, N 2.61; Found: C 53.52, H 6.562, N 2.63.

[Mo(N-2,6-*i*Pr₂-C₆H₃)(CHCMe₂Ph)Br₂(CAAC)] (Mo7): **Mo3** (150 mg, 0.23 mmol, 1 equiv.) was dissolved in benzene, a solution of CAAC (containing 1 equiv. of HMDS, 103 mg, 0.23 mmol, 1 equiv.) in benzene was added and the reaction mixture was stirred for 1 h at room temperature. All volatiles were removed *in vacuo* and co-evaporated with pentane. The foam was taken up in a small amount of diethyl ether, filtered and the solution was placed in a freezer (-35 °C) overnight to get shiny yellow crystals. The product was isolated as a mixture of two isomers in a 9:1 ratio. Due to the low abundance of the minor isomer, only the characteristic signals for the main isomer are reported. Yield: 127 mg (65%). ¹H NMR (C₆D₆): δ 10.61 (s, minor isomer), 10.43 (s, 1H, major isomer), 7.29 (dd, 2H, J = 8), 7.26 (t, 1H), 7.07-7.04 (m, 5H), 6.98 (s, 3H), 4.71 (sept, 2H, J = 6.6), 3.40 (sept, 2H, J = 8), 1.83 (s, 6H), 1.66 (s, 6H), 1.46 (s,

2H), 1.43 (d, $J=4$, 6H), 1.41 (d, $J=8$, 12H), 1.15 (d, $J=4$, 6H), 0.95 (s, 6H); $^{13}\text{C NMR}$ (C_6D_6): δ 310.2 (CHCMe_2Ph , minor isomer), 300.2 (CHCMe_2Ph , major isomer), 268.2 ($\text{C}_{\text{carbonyl}}$ major isomer), 263.0 ($\text{C}_{\text{carbonyl}}$ minor isomer), 152.8, 148.3, 148.1, 147.5, 135.5, 129.9, 128.3, 127.2, 126.7, 126.4, 126.1, 124.2, 82.2, 56.2, 54.5, 52.3, 33.6, 29.8, 29.8, 29.6, 29.0, 28.9, 25.9, 25.8. Elemental Analysis Calculated for $\text{C}_{42}\text{H}_{60}\text{Br}_2\text{MoN}_2\text{C}$, 59.44; H, 7.13; N, 3.30; Found: C, 59.57; H, 7.19; N, 3.18.

[Mo(N-2-tBuC₆H₄)(CHCMe₂Ph)Cl₂(CAAC)] (Mo9): A solution of CAAC (containing 1 equiv. HMDS, 125 mg, 0.28 mmol, 1 equiv.) in benzene was added to a solution of **Mo6** (150 mg, 0.28 mmol, 1 equiv.) in benzene. The resulting red solution was stirred at room temperature for 1 h and the solvent was removed *in vacuo*. The residue was recrystallized from a mixture of CH_2Cl_2 and *n*-pentane. Yield: 122 mg (60%). $^1\text{H NMR}$ (C_6D_6) δ 10.60 (s, 1H), 8.72 (dd, $J=8.0$, 1.5, 1H), 7.40–7.37 (m, 3H), 7.33–7.29 (m, 3H), 7.23–7.12 (m, 4H), 7.05 (td, $J=7.6$, 1.6, 1H), 3.39 (hept, $J=6.5$, 2H), 1.89 (s, 15H), 1.77 (s, 6H), 1.61 (s, 2H), 1.55 (d, $J=6.3$, 6H), 1.30 (d, $J=6.5$, 6H), 1.10 (s, 6H); $^{13}\text{C NMR}$ (C_6D_6) δ 296.9, 267.4, 155.5, 148.2, 147.8, 144.6, 135.4, 129.9, 129.8, 126.7, 126.7, 126.5, 126.2, 126.0, 125.8, 81.7, 56.0, 55.1, 52.0, 35.9, 32.2, 30.7, 30.1, 29.5, 29.1, 28.7, 25.7. Elemental Analysis (%) Calcd. for $\text{C}_{40}\text{H}_{56}\text{Cl}_2\text{MoN}_2$: C, 65.66; H, 7.71; N, 3.83; Found: C, 65.55; H, 7.729; N, 3.84.

[Mo(N-2,6-iPr-C₆H₃)(CHCMe₂Ph)Br(CAAC)][B(Ar^F)₄] (Mo10): A solution of **Mo7** (125 mg, 0.15 mmol, 1 equiv.) in diethyl ether was added to a solution of $\text{NaB}(\text{Ar}^{\text{F}})_4$ (130.4 mg, 0.15 mmol, 1 equiv.) in diethyl ether and stirred for 1 h at room temperature. The solution was filtered over celite and the filtrate was dried *in vacuo* to yield an orange solid. The product was recrystallized from a mixture of diethyl ether and pentane. Two molecules of diethyl ether cocrystallized. Yield: 180 mg (75%, product obtained in two crops). $^1\text{H NMR}$ (CDCl_3): δ 12.47 (s, 1H), 7.72 (brs, 8H), 7.67 (t, $J=6\text{H}$, 1H), 7.53 (brs, 4H), 7.41–7.38 (m, 2H), 7.36–7.30 (m, 5H), 7.26–7.23 (m, 1H), 7.21 (s, 1H), 7.19 (s, 1H), 3.38 (sept, $J=8$, 2H), 2.78 (sept, $J=7$, 1H), 2.62 (sept, $J=7$, 1H), 2.10 (s, 2H), 1.78 (s, 3H), 1.62 (s, 3H), 1.53 (s, 3H), 1.36 (s, 3H), 1.35 (s, 3H), 1.34 (d, $J=8$, 3H), 1.31 (d, $J=8$, 3H), 1.24 (d, $J=8$, 3H), 1.18 (d, $J=4\text{H}, 6\text{H}$), 1.15 (d, $J=8$, 3H), 1.12 (d, $J=8$, 6H), 0.90 (s, 3H); $^{19}\text{F NMR}$ (CDCl_3): δ –62.36 (s, 24F); $^{13}\text{C NMR}$ (CDCl_3) δ 305.6, 252.9, 162.0 (q, $J_{\text{BC}}=50$, $\text{B}(\text{Ar}^{\text{F}})_4$), 155.1, 147.6, 147.0, 146.3, 144.5, 135.1, 134.5, 131.7, 129.4, 129.2 (qq, $J_{\text{CF}}=31.7$, $J_{\text{CB}}=2.8$, $\text{B}(\text{Ar}^{\text{F}})_4$), 129.0, 128.7, 128.1, 127.8, 125.8, 125.1, 124.9 (q, $J_{\text{CF}}=273.0$, $\text{B}(\text{Ar}^{\text{F}})_4$), 117.8 (m, $\text{B}(\text{Ar}^{\text{F}})_4$), 86.1, 58.7, 56.9, 50.1, 31.3, 31.0, 30.7, 29.6, 29.6, 29.5, 29.5, 28.7, 27.6, 27.1, 27.0, 26.3, 26.0, 24.4, 23.6. Despite numerous efforts, the high sensitivity of this compound to air and moisture did not allow for satisfactory elemental analysis.

[Mo(N-2-CF₃-C₆H₄)(CHCMe₂Ph)Br₂(CAAC)] (Mo8) and [Mo(N-2-CF₃-C₆H₄)(CHCMe₂Ph)Br(CAAC)][B(Ar^F)₄] (Mo11): **Mo4** (60 mg, 0.094 mmol, 1 equiv.) was dissolved in benzene, a solution of CAAC (containing 1 equiv. of HMDS, 42.1 mg, 0.094 mmol, 1 equiv.) in benzene was added and the reaction mixture was stirred for 1 h at room temperature. All volatiles were removed *in vacuo* and co-evaporated with pentane. The residue was then washed with pentane to obtain yellow crude **Mo8** (70 mg, 0.084 mmol), which was again suspended in diethyl ether. A solution of $\text{NaB}(\text{Ar}^{\text{F}})_4$ (74.5 mg, 0.084 mmol, 0.9 equiv.) in diethyl ether was added and the mixture was stirred for 1 h at room temperature. The solution was filtered through celite and the filtrate was dried *in vacuo* to yield a solid, which was recrystallized from a mixture of CH_2Cl_2 and pentane. Half a molecule of CH_2Cl_2 was trapped along with the product and did not evaporate even under high vacuum. Yield: 100 mg (64% with respect to **Mo4**). $^1\text{H NMR}$ (CDCl_3): δ 11.99 (s, 1H), 7.73 (t, $J=8$, 1H), 7.71 (br s, 8H), 7.67–7.65 (m, 1H), 7.52 (brs, 4H), 7.49–7.45 (m, 3H), 7.41 (dd, $J=8$, 1H), 7.26–7.15 (m, 5H), 7.11–7.07 (m, 1H), 5.30 (s, 1H, CH_2Cl_2), 2.92 (sept, $J=6$, 1H), 2.50 (sept, $J=7$, 1H), 2.09 (d, $J=4$, 2H), 1.60 (s, 6H), 1.59 (s, 3H), 1.59 (d, $J=8$, 3H),

1.37 (d, $J=4$, 3H), 1.29–1.26 (m, 12H), 1.22 (d, $J=8$, 3H); $^{19}\text{F NMR}$ (CDCl_3): δ –59.05 (3F), –62.34 (24F); $^{13}\text{C NMR}$ (CDCl_3): δ 305.1, 259.2, 161.8 (q, $J_{\text{BC}}=49.9$, $\text{B}(\text{Ar}^{\text{F}})_4$), 152.5, 148.0, 145.7, 143.6, 134.9, 134.7, 133.0, 130.7, 130.4, 129.3, 129.1, 129.0 (qq, $J_{\text{CF}}=31.7$, $J_{\text{CB}}=2.9$, $\text{B}(\text{Ar}^{\text{F}})_4$), 128.10, 127.02(m), 127.0, 126.7, 126.0, 124.7 (q, $J_{\text{CF}}=272.5$, $\text{B}(\text{Ar}^{\text{F}})_4$), 122.3, 117.6 (m, $\text{B}(\text{Ar}^{\text{F}})_4$), 84.4, 59.5, 57.0, 53.6 (CH_2Cl_2), 51.0, 30.8, 29.8, 29.9, 29.5, 29.4, 29.2, 29.1, 28.8, 27.6, 26.4, 26.1, 23.7. Elemental Analysis Calculated for $\text{C}_{69}\text{H}_{59}\text{BrF}_2\text{BMoN}_2\text{O}.5\text{CH}_2\text{Cl}_2$: C, 50.34; H, 3.65; N, 1.69; Found: C, 50.43; H, 3.82; N, 1.63.

[Mo(N-2-tBu-C₆H₄)(CHCMe₂Ph)Cl(CAAC)][B(Ar^F)₄] (Mo12): A solution of **Mo9** (71 mg, 0.097 mmol) in CH_2Cl_2 was added to a solution of $\text{NaB}(\text{Ar}^{\text{F}})_4$ (86 mg, 0.097 mmol, 1 equiv.) in CH_2Cl_2 and the mixture was stirred for 1 h at room temperature. The solution was filtered and dried *in vacuo*. The product was recrystallized from a mixture of CH_2Cl_2 , diethyl ether and pentane. Yield: 132 mg (87%). $^1\text{H NMR}$ (CDCl_3): δ 12.19 (s, 1H), 7.71 (brm, 8H), 7.69 (m, 1H), 7.53 (brs, 4H), 7.52–7.49 (m, 2H), 7.43 (q, 2H), 7.32 (t, 1H, $J=8$), 7.27–7.15 (m, 6H), 2.98 (sept, 1H, $J=7$), 2.50 (sept, 1H, $J=6$), 2.11 (s, 2H), 1.68 (s, 3H), 1.62 (s, 3H), 1.58 (s, 3H), 1.54 (d, $J=4$, 3H), 1.43 (s, 9H), 1.42 (s, 3H), 1.37 (d, $J=4$, 3H), 1.33 (s, 3H), 1.27 (d, $J=8$, 3H), 1.23 (s, 3H), 1.22 (d, 3H); $^{19}\text{F NMR}$ (CDCl_3): δ –62.34 (24F); $^{13}\text{C NMR}$ (CDCl_3) δ 304.5, 262.8, 161.8 (q, q, $J_{\text{BC}}=49.9$, $\text{B}(\text{Ar}^{\text{F}})_4$), 156.9, 148.3, 148.2, 145.4, 144.1, 135.0, 134.5, 134.0, 131.9, 129.1, 129.1, 129.0 (qq, $J_{\text{CF}}=31.7$, $J_{\text{CB}}=2.9$, $\text{B}(\text{Ar}^{\text{F}})_4$), 129.0, 128.1, 127.7, 127.4, 127.0, 125.6, 124.7 (q, $J_{\text{CF}}=272.8$, $\text{B}(\text{Ar}^{\text{F}})_4$), 117.6 (m, $\text{B}(\text{Ar}^{\text{F}})_4$), 85.0, 60.0, 57.6, 51.9, 36.1, 31.5, 30.8, 30.7, 30.6, 30.4, 29.5, 29.3, 29.0, 28.2, 28.0, 25.7, 25.2, 23.3. Elemental Analysis Calculated for $\text{C}_{72}\text{H}_{68}\text{BClF}_{24}\text{MoN}_2$: C, 55.45; H, 4.40; N, 1.80; Found: C, 55.43; H, 4.44; N, 1.77.

[Mo(N-2-tBu-C₆H₄)(CHCMe₂Ph)Cl(CAAC)(CH₃CN)][B(Ar^F)₄] (Mo12CH₃CN): A solution of **Mo9** (300 mg, 402 μmol , 1 equiv.) in CH_2Cl_2 was added to a solution of $\text{Na}(\text{BAr}^{\text{F}})_4$ (356 mg, 402 μmol , 1 equiv.) in CH_2Cl_2 . The suspension was stirred for 1 h at room temperature, filtered through celite, and a few drops of CH_3CN were added. The color changed from yellow to pale orange. The solvent was evaporated and the product was obtained as yellow solid. Yield: 638 mg (98%). Single crystals suitable for X-ray analysis were obtained from a mixture of CH_2Cl_2 and pentane. $^1\text{H NMR}$ (CDCl_3): δ 11.93 (s, 1H), 7.71 (brs, 8H), 7.55 (brs, 1H), 7.52 (br s, 4H), 7.45 (d, $J=8$, 2H), 7.36 (brs, 2H), 7.28–7.21 (m, 4H), 7.16 (s, 2H), 7.01 (brs, 2H), 3.62 (sept*, 1H), 2.63 (sept*, 1H), 2.05 (s, 2H), 1.83 (s, 3H), 1.73 (s, 6H), 1.57 (d, $J=8$, 6H), 1.45 (s, 12H), 1.35 (d, $J=4$, 6H), 1.24 (s, 3H), 1.05 (s, 3H), 0.66 (s, 3H). $^{19}\text{F NMR}$ (CDCl_3): δ –62.37 (24F); $^{13}\text{C NMR}$ (CDCl_3) δ 323.4, 257.8, 161.9 (q, $J_{\text{BC}}=49.9$, $\text{B}(\text{Ar}^{\text{F}})_4$), 155.4, 147.5, 145.8, 144.7, 143.7, 137.5, 135.0, 132.5, 131.4, 130.5, 129.0 (qq, $J_{\text{CF}}=31.7$, $J_{\text{CB}}=2.9$, $\text{B}(\text{Ar}^{\text{F}})_4$), 128.8, 127.3, 127.2, 126.8, 126.6, 126.4, 126.0, 124.7 (q, $J_{\text{CF}}=272.8$, $\text{B}(\text{Ar}^{\text{F}})_4$), 117.6 (m, $\text{B}(\text{Ar}^{\text{F}})_4$), 83.5, 59.1, 58.5, 51.6, 36.3, 32.6, 31.1, 30.6, 30.5, 29.3, 29.3, 28.2, 27.7, 27.1, 26.3, 26.1, 22.9, 2.8. Elemental Analysis Calculated for $\text{C}_{74}\text{H}_{71}\text{BClF}_{24}\text{MoN}_3$: C, 55.53; H, 4.47; N, 2.63; Found: C, 55.56; H, 4.45; N, 2.53. *The terminal signals of the septet were poorly resolved.

[Mo(N-2,6-iPr-C₆H₃)(CHCMe₂Ph)(OTf)(CAAC)][B(Ar^F)₄] (Mo15): A solution of **Mo10** (60 mg, 0.037 mmol) in CH_2Cl_2 was added to solid silver triflate (14.2 mg, 0.055 mmol, 1.5 equiv.). The suspension was stirred for 2 h at ambient temperature and the color changed from orange to yellow. The precipitate was filtered off and the filtrate was concentrated, pentane was added and the mixture was stored at -35°C to get yellow crystals. One molecule of CH_2Cl_2 cocrystallized. Yield: 40 mg (76%). $^1\text{H NMR}$ (CDCl_3): δ 13.20 (s, 1H), 7.71 (br s, 8H), 7.71–7.68 (m, 1H), 7.52 (brs, 4H), 7.47 (t, $J=8$, 2H), 7.41 (t, 1H, $J=8$), 7.37–7.31 (m, 4H), 7.29–7.24 (m, 3H), 3.07 (sept, 2H, $J=6$), 2.87 (sept, $J=7$, 1H), 2.47 (sept, $J=7$, 1H), 2.11 (d, $J=8$, 2H), 1.81 (s, 3H), 1.64 (d, 6H, $J=20$), 1.32 (s, 3H), 1.30–1.27 (m, 6H, $J=8$), 1.26 (s, 3H), 1.24 (s, 6H), 1.15 (d, 3H), 1.14 (d, 6H), 0.95 (d, 3H, $J=4$), 0.73 (s, 3H). $^{19}\text{F NMR}$ (CDCl_3): δ –62.36 (s, 24F), –74.66 (s, 3F); $^{13}\text{C NMR}$ (CD_2Cl_2): δ 316.4, 250.2, 162.3 (q, $J_{\text{BC}}=49.9$, $\text{B}(\text{Ar}^{\text{F}})_4$), 156.0, 149.1, 146.5, 144.1,

135.4, 133.4, 130.2, 129.8, 129.4 (qq, $^2J_{CF}=31.7$, $^3J_{CB}=2.8$, B(Ar^F)₄), 128.6, 128.5, 126.4, 125.7, 125.2 (q, $^1J_{CF}=272.5$, B(Ar^F)₄), 119.1 (q, $^1J_{CF}=318.5$ MHz, CF₃SO₃), 118.04 (m, B(Ar^F)₄), 86.0, 60.6, 60.0, 51.2, 32.6, 31.1, 31, 30.1, 30.0, 30.0, 29.1, 28.6, 26.6, 25.9, 25.2, 23.9, 23.9, 23.8. Elemental Analysis Calculated for C₇₅H₇₂BF₂₇MoN₂O₃S: C, 52.95; H, 4.27; N, 1.65; Found: C, 52.96; H, 4.48; N, 1.66.

[Mo(N-2-*t*Bu-C₆H₄)(CHCMe₂Ph)(OTf)(CAAC)(CH₃CN)] [B(Ar^F)₄] (Mo16): A solution of Mo12-CH₃CN (70 mg, 0.044 mmol) was added to solid silver triflate (16.86 mg, 0.065 mmol, 1.5 equiv.) and the suspension was stirred for 2 h at room temperature. The precipitate was filtered off, the filtrate was concentrated and few drops of pentane were added and stored at -35 °C to get yellow crystals. Yield: 70 mg (93%). ¹H NMR (CDCl₃): δ 12.34 (s, 1H), 7.71 (brs, 8H), 7.63-7.56 (m, 2H), 7.51 (brs, 4H), 7.48 (dd, *J*=8, 1H), 7.39 (t, *J*=8, 2H), 7.31 (t, *J*=8, 1H), 7.28-7.24 (m, 2H), 7.19-7.13 (m, 2H), 7.03-7.00 (m, 2H), 3.29 (sept, *J*=6, 1H), 2.61 (sept, *J*=7, 1H), 2.06 (d, *J*=4, 2H), 1.85 (s, 3H), 1.77 (s, 3H), 1.65 (s, 3H), 1.59 (s, 3H), 1.57 (d, *J*=4, 3H), 1.48 (s, 9H), 1.42 (d, *J*=4, 3H), 1.39 (d, *J*=8, 3H), 1.34 (d, *J*=8, 3H), 1.30 (s, 3H), 1.14 (s, 3H), 0.68 (s, 3H); ¹⁹F NMR (CDCl₃): δ -62.38 (s, 24F), -76.30 (s, 3F); ¹³C NMR (CDCl₃): δ 323.2, 256.0, 161.9 (q, $^1J_{BC}=49.9$, B(Ar^F)₄), 155.6, 148.8, 145.4, 144.6, 142.1, 136.6, 135.0, 133.8, 131.8, 131.8, 129.1 (qq, $^2J_{CF}=31.7$, $^3J_{CB}=2.8$, B(Ar^F)₄), 129.0, 127.7, 127.5, 127.1, 127.0, 126.9, 126.7, 126.3, 124.7 (q, $^1J_{CF}=272.5$, B(Ar^F)₄), 119.2 (q, $^1J_{CF}=318.5$ MHz, CF₃SO₃), 117.6 (m, B(Ar^F)₄), 85.8, 59.8, 59.1, 50.3, 36.2, 33.0, 31.7, 31.1, 29.3, 28.9, 28.6, 28.1, 28.0, 27.2, 26.9, 26.9, 26.5, 22.6, 3.0. Elemental Analysis Calculated for C₇₅H₇₁F₂₇BMoN₃O₃S: C, 52.55; H, 4.18; N, 2.45; Found: C, 52.51; H, 4.27; N, 2.51.

[Mo(N-2,6-*i*Pr-C₆H₃)(CHCMe₂Ph)(OC₆F₅)(CAAC)][B(Ar^F)₄] (Mo17): A solution of Mo10 (50.0 mg, 0.031 mmol) in CH₂Cl₂ was added to a solution of lithium pentafluorophenoxide (8.7 mg, 0.046 mmol, 1.5 equiv.) in CH₂Cl₂. The suspension was stirred for 2 h at ambient temperature and the color changed from orange to yellow. The precipitate was filtered off, the filtrate was concentrated and pentane was added and the mixture stored at -35 °C to allow the product to crystallize. Yield: 45 mg (86%). ¹H NMR (CDCl₃): δ 13.45 (s, 1H), 7.73 (brs, 8H), 7.54 (brs, 4H), 7.49-7.42 (m, 2H), 7.36-7.33 (m, 5H), 7.27-7.18 (m, 4H), 3.15 (sept, *J*=6, 2H), 2.73 (sept, *J*=4, 2 H), 2.11 (brs, 2H), 1.92 (s, 3H), 1.54 (s, 3H), 1.48 (s, 3H), 1.39 (s, 3H), 1.37 (s, 3H), 1.36 (d, *J*=8, 3H), 1.26 (dd, 6H), 1.15 (d, *J*=4, 3H), 1.13 (d, *J*=8, 6H), 1.04 (d, *J*=8, 6H), 0.79 (s, 3H); ¹⁹F NMR (CDCl₃): δ -62.37 (24F), -156.68 (d, 2F), -163.02 (t, 2F), -163.86 (t, 1F); ¹³C NMR (CDCl₃): δ 308.8, 256.6, 161.9 (q, $^1J_{BC}=49.9$, B(Ar^F)₄), 154.2, 147.2, 147.0, 146.0, 144.2, 140.6, 139.2, 138.6, 137.3, 135.9, 135.0, 133.3, 131.7, 130.3, 129.2, 129.0 (qq, $^2J_{CF}=31.7$, $^3J_{CB}=2.8$, B(Ar^F)₄), 128.2, 128.0, 127.0, 125.6, 124.7 (q, $^1J_{CF}=272.5$, B(Ar^F)₄), 124.7, 117.6 (m, B(Ar^F)₄), 85.7, 58.5, 57.0, 50.3, 31.0, 30.7, 29.8, 29.6, 29.3, 29.3, 28.6, 27.8, 27.8, 26.8, 26.6, 25.4, 24.7, 24.0, 23.8; Elemental Analysis Calculated for C₈₀H₇₂BF₂₉MoN₂O: C, 55.38; H, 4.18; N, 1.61; Found: C, 55.09; H, 4.34; N, 1.54.

[Mo(N-2-*t*Bu-C₆H₄)(CHCMe₂Ph)(OC₆F₅)(CAAC)][B(Ar^F)₄] (Mo18): A solution of Mo12-CH₃CN (70 mg, 0.044 mmol) in CH₂Cl₂ was added to a solution of lithium pentafluorophenoxide (12.45 mg, 0.066 mmol, 1.5 equiv.) in CH₂Cl₂. The suspension was stirred for 2 h at ambient temperature. A precipitate formed and was filtered off, the filtrate was concentrated, pentane was added and the mixture was stored at -35 °C to allow the product to crystallize. Yield: 60 mg (80%). ¹H NMR (CDCl₃): δ 13.19 (s, 1H), 7.70 (brs, 8H), 7.52 (brs, 4H), 7.47 (dd, *J*=4, 1H), 7.43 (t, *J*=8, 2H), 7.36-7.31 (m, 2H), 7.28-7.26 (m, 2H), 7.25-7.19 (m, 5H), 3.04 (sept, *J*=7, 1H), 2.53 (sept, *J*=6, 1H), 2.09 (d, *J*=8, 2H), 1.79 (s, 3H), 1.65 (d, *J*=4, 3H), 1.58 (s, 3H), 1.51 (s, 3H), 1.44 (s, 3H), 1.33-1.28 (m, 9H) 1.24 (s, 3H), 1.22 (s, 3H), 1.19 (s, 9H); ¹⁹F NMR (CDCl₃): δ -62.38 (24F), -158.09 (d, 2F), -163.12 (t, 2F), -164.97 (t, 1F); ¹³C NMR (CD₂Cl₂): δ 310.1, 266.8, 162.6 (q, $^1J_{BC}=49.9$, B(Ar^F)₄), 157.0, 149.5, 149.2, 145.5, 144.9, 140.6, 139.2, 137.8, 137.3, 135.9, 135.4, 133.7, 133.1, 131.9, 131.6, 129.4

(qq, $^2J_{CF}=31.1$, $^3J_{CB}=2.8$, B(Ar^F)₄), 129.4, 129.1, 128.4, 127.8, 127.5, 126.3, 125.2 (q, $^1J_{CF}=272.5$, B(Ar^F)₄), 118.1 (m, B(Ar^F)₄), 85.0, 60.6, 58.3, 52.6, 35.8, 32.2, 31.6, 30.7, 30.1, 30.0, 30.0, 29.8, 29.6, 29.0, 27.9, 26.1, 24.7, 23.7. Elemental Analysis Calculated for C₇₈H₆₈BF₂₉MoN₂O: C, 54.88; H, 4.02; N, 1.64; Found: C, 54.61; H, 4.06; N, 1.74.

Computational details: Complexes Mo-16 and Mo-19 were optimized using density functional theory (DFT) starting from the single-crystal X-ray structure for Mo-16, while geometry optimization for Mo-19 was started from Mo-16 after replacing the CAAC ligand by the NHC ligand. Geometry optimizations of the two complexes were performed using the hybrid functional PBE0^[20] and the def2-SVP basis set,^[21] including empirical dispersion corrections via Grimme's DFT-D3 version with Becke-Johnson damping (D3BJ).^[22] Partial charge distributions were obtained from the calculation of population analysis at PBE0-D3BJ/def2-TZVP level using the PBE0-D3BJ/def2-SVP-optimized geometries. Natural population analysis (NPA).^[23] Hirshfeld^[24] and charge model 5 (CM5)^[25] charges were calculated. All three charge models showed similar results; thus, only the CM5 results are discussed in the main article. All calculations were performed in Gaussian 16 (revision C.01).^[26]

Acknowledgements

Financial support provided by the Deutsche Forschungsgemeinschaft DFG (German Research Foundation, projects ID 358283783 – CRC 1333/2 2022, BU 2174/24-1, INST 40/575-1 FUGG – JUSTUS 2 cluster) and by the state of Baden-Württemberg through bwHPC is gratefully acknowledged. Open Access funding enabled and organized by Projekt DEAL.

Conflict of Interests

The authors declare no conflict of interest.

Data Availability Statement

The data that support the findings of this study are available from the corresponding author upon reasonable request.

Keywords: alkylidene · cyclic alkyl amino carbenes · halides · molybdenum · olefin metathesis

- [1] a) K. V. Bukhryakov, R. R. Schrock, A. H. Hoveyda, C. Tsay, P. Muller, *J. Am. Chem. Soc.* **2018**, *140*, 2797–2800; b) A. D. Horton, R. R. Schrock, *Polyhedron* **1988**, *7*, 1841–1853; c) A. S. Hock, R. R. Schrock, A. H. Hoveyda, *J. Am. Chem. Soc.* **2006**, *128*, 16373–16375; d) R. R. Schrock, *Chem. Rev.* **2009**, *109*, 3211–3226.
- [2] a) D. R. Anderson, T. Ung, G. Mkrtumyan, G. Bertrand, R. H. Grubbs, Y. Schrodi, *Organometallics* **2008**, *27*, 563–566; b) D. Martin, V. M. Marx, R. H. Grubbs, G. Bertrand, *Adv. Synth. Catal.* **2016**, *358*, 965–969; c) T. S. Ahmed, J. M. Grandner, B. L. H. Taylor, M. B. Herbert, K. N. Houk, R. H. Grubbs, *Organometallics* **2018**, *37*, 2212–2216; d) Y. Xu, J. J. Wong, A. E. Samkian, J. H. Ko, S. Chen, K. N. Houk, R. H. Grubbs, *J. Am. Chem. Soc.* **2020**, *142*, 20987–20993.
- [3] M. K. Samantaray, V. D'Elia, E. Pump, L. Falivene, M. Harb, S. Ould Chikh, L. Cavallo, J. M. Basset, *Chem. Rev.* **2020**, *120*, 734–813.
- [4] a) C. Coperet, A. Comas-Vives, M. P. Conley, D. P. Estes, A. Fedorov, V. Mougél, H. Nagae, F. Nunez-Zarur, P. A. Zhizhko, *Chem. Rev.* **2016**, *116*,

- 323–421 ; b) F. Blanc, C. Coperet, A. Lesage, L. Emsley, *Chem. Soc. Rev.* **2008**, *37*, 518–526.
- [5] a) M. J. Benedikter, J. V. Musso, W. Frey, R. Schowner, M. R. Buchmeiser, *Angew. Chem. Int. Ed.* **2021**, *60*, 1374–1382 ; b) P. M. Hauser, K. Gugeler, W. Frey, J. Kästner, M. R. Buchmeiser, *Organometallics* **2021**, *40*, 4026–4034 ; c) M. R. Buchmeiser, S. Sen, C. Lienert, L. Widmann, R. Schowner, K. Herz, P. Hauser, W. Frey, D. Wang, *ChemCatChem* **2016**, *8*, 2710–2723 ; d) I. Elser, R. Schowner, W. Frey, M. R. Buchmeiser, *Chem. Eur. J.* **2017**, *23*, 6398–6405 ; e) M. J. Benedikter, R. Schowner, I. Elser, P. Werner, K. Herz, L. Stöhr, D. A. Imbrich, G. M. Nagy, D. Wang, M. R. Buchmeiser, *Macromolecules* **2019**, *52*, 4059–4066 ; f) J. V. Musso, V. Gramm, S. Stein, W. Frey, M. R. Buchmeiser, *Eur. J. Inorg. Chem.* **2022**, *26* ; g) R. R. Schrock, M. R. Buchmeiser, J. Groos, M. J. Benedikter, *Comprehensive Organometallic Chemistry IV (4th Ed.)* **2022**, *5*, 671–773 ; h) M. J. Benedikter, F. Ziegler, J. Groos, P. M. Hauser, R. Schowner, M. R. Buchmeiser, *Coord. Chem. Rev.* **2020**, *415*, 213315.
- [6] V. Lavallo, Y. Canac, C. Prasang, B. Donnadiou, G. Bertrand, *Angew. Chem. Int. Ed.* **2005**, *44*, 5705–5709.
- [7] M. Soleilhavou, G. Bertrand, *Acc. Chem. Res.* **2015**, *48*, 256–266.
- [8] Y. Gao, S. Yazdani, A. T. Kendrick, G. P. Junor, T. Kang, D. B. Grotjahn, G. Bertrand, R. Jazzar, K. M. Engle, *Angew. Chem. Int. Ed.* **2021**, *60*, 19871–19878.
- [9] M. T. Proetto, K. Alexander, M. Melaimi, G. Bertrand, N. C. Gianneschi, *Chem. Eur. J.* **2021**, *27*, 3772–3778.
- [10] a) K. Kaczanowska, B. Trzaskowski, A. Peszczyńska, A. Tracz, R. Gawin, T. K. Olszewski, K. Skowerski, *ChemCatChem* **2020**, *12*, 6366–6374 ; b) A. E. Samkian, Y. Xu, S. C. Virgil, K.-Y. Yoon, R. H. Grubbs, *Organometallics* **2020**, *39*, 495–499.
- [11] H. H. Fox, K. B. Yap, J. Robbins, S. Cai, R. R. Schrock, *Inorg. Chem.* **1992**, *31*, 2287–2289.
- [12] U. S. D. Paul, C. Sieck, M. Haehnel, K. Hammond, T. B. Marder, U. Radius, *Chem. Eur. J.* **2016**, *22*, 11005–11014.
- [13] M. J. Benedikter, J. V. Musso, W. Frey, R. Schowner, M. R. Buchmeiser, *Angew. Chem. Int. Ed.* **2021**, *60*, 1374–1382.
- [14] R. Schowner, W. Frey, M. R. Buchmeiser, *Eur. J. Inorg. Chem.* **2019**, *2019*, 1911–1922.
- [15] a) K. V. Bukhryakov, S. VenkatRamani, C. Tsay, A. Hoveyda, R. R. Schrock, *Organometallics* **2017**, *36*, 4208–4214 ; b) M. J. Kohl, T. T. Nguyen, J. M. Lam, S. Torker, J. Hyvl, R. R. Schrock, A. Hoveyda, *Nature* **2017**, *542*, 80–86 ; c) J. K. Lam, C. Zhu, K. V. Bukhryakov, P. Müller, A. Hoveyda, R. R. Schrock, *J. Am. Chem. Soc.* **2016**, *138*, 15774–15783.
- [16] I. Elser, M. J. Benedikter, R. Schowner, W. Frey, D. R. Wang, M. R. Buchmeiser, *Organometallics* **2019**, *38*, 2461–2471 *Organometallics*.
- [17] A. W. Addison, T. N. Rao, J. Reedijk, J. van Rijn, G. C. Verschoor, *J. Chem. Soc. Dalton Trans.* **1984**, 1349–1356.
- [18] R. Schowner, I. Elser, M. Benedikter, M. Momin, W. Frey, T. Schneck, L. Stohr, M. R. Buchmeiser, *Angew. Chem. Int. Ed.* **2020**, *59*, 951–958.
- [19] C. Müller, D. M. Andrada, I.-A. Bischoff, M. Zimmer, V. Huch, N. Steinbrück, A. Schäfer, *Organometallics* **2019**, *38*, 1052–1061.
- [20] C. Adamo, V. Barone, *J. Chem. Phys.* **1999**, *110*, 6158–6170.
- [21] F. Weigend, R. Ahlrichs, *Phys. Chem. Chem. Phys.* **2005**, *7*, 3297–3305.
- [22] a) S. Grimme, J. Antony, S. Ehrlich, H. Krieg, *J. Chem. Phys.* **2010**, *132*, 154104 ; b) S. Grimme, S. Ehrlich, L. Goerigk, *J. Comput. Chem.* **2011**, *32*, 1456–1465.
- [23] A. E. Reed, R. B. Weinstock, F. Weinhold, *J. Chem. Phys.* **1985**, *83*, 735–746.
- [24] a) F. L. Hirshfeld, *XVII. Spatial Partitioning of Charge Density* **1977**, *16*, 198–201 ; b) F. L. Hirshfeld, *Theor. Chim. Acta* **1977**, *44*, 129–138.
- [25] A. V. Marenich, S. V. Jerome, C. J. Cramer, D. G. Truhlar, *J. Chem. Theory Comput.* **2012**, *8*, 527–541.
- [26] M. J. Frisch, G. W. Trucks, H. B. Schlegel, G. E. Scuseria, M. A. Robb, J. R. Cheeseman, G. Scalmani, V. Barone, G. A. Petersson, H. Nakatsuji, X. Li, M. Caricato, A. V. Marenich, J. Bloino, B. G. Janesko, R. Gomperts, B. Mennucci, H. P. Hratchian, J. V. Ortiz, A. F. Izmaylov, J. L. Sonnenberg, D. Williams-Young, F. Ding, F. Lipparini, F. Egidi, J. Goings, B. Peng, A. Petrone, T. Henderson, D. Ranasinghe, V. G. Zakrzewski, J. Gao, N. Rega, G. Zheng, W. Liang, M. Hada, M. Ehara, K. Toyota, R. Fukuda, J. Hasegawa, M. Ishida, T. Nakajima, Y. Honda, O. Kitao, H. Nakai, T. Vreven, K. Throssell, J. A. J. Montgomery, J. E. Peralta, F. Ogliaro, M. Bearpark, J. J. Heyd, E. N. Brothers, K. N. Kudin, V. N. Staroverov, R. Kobayashi, J. Normand, K. Raghavachari, A. Rendell, J. C. Burant, S. S. Iyengar, J. Tomasi, M. Cossi, J. M. Millam, M. Klene, C. Adamo, R. Cammi, J. W. Ochterski, R. L. Martin, K. Morokuma, O. Farkas, J. B. Foresman, D. J. Fox, *Gaussian 16, revision C.01; Gaussian, Inc.: Wallingford CT* **2016**.

Manuscript received: June 6, 2023

Accepted manuscript online: June 27, 2023

Version of record online: August 9, 2023